International Journal of Energy Research

INTERNATIONAL JOURNAL OF ENERGY RESEARCH
Int. J. Energy Res. 2013; **37**:1223–1231
Published online 17 May 2012 in Wiley Online Library (wileyonlinelibrary.com). DOI: 10.1002/er.2920

Effect of time-varying humidity on the performance of polymer electrolyte membrane fuel cells

Shamsuddin Noorani[1] and Tariq Shamim[2,*,†]

[1]Department of Mechanical Engineering, The University of Michigan-Dearborn, Dearborn, MI, USA
[2]Mechanical Engineering, Masdar Institute of Science and Technology, Abu Dhabi, United Arab Emirates

SUMMARY

This paper presents a computational investigation of the effect of time-varying humidity conditions on a polymer electrolyte membrane fuel cell. The objective is to develop a better fundamental understanding of the fuel cell's performance under actual driving conditions. Such an understanding will be beneficial in improving the fuel cell design for mobile applications. The study employs a macroscopic single-fuel cell-based, one-dimensional, isothermal model. The novelty of the model is that it does not rely on the non-physical assumption of the uptake curve equilibrium between the pore vapor and ionomer water in the catalyst layers. Instead, the transition between the two phases is modeled as a finite-rate equilibration process. The modulating conditions are simulated by forcing the temporal variations in reactant humidity. The results show that reactant humidity modulations cause a departure in the cell behavior from its steady behavior, and the finite-rate equilibration between the catalyst vapor and liquid water can be a factor in determining the cell response. The cell response is also affected by the modulating frequency and amplitude. Copyright © 2012 John Wiley & Sons, Ltd.

KEY WORDS

fuel cell; humidity; water distribution; dynamic behavior; modeling and simulations

Correspondence

*Tariq Shamim, Professor of Mechanical Engineering, Masdar Institute of Science and Technology, Abu Dhabi, United Arab Emirates
†E-mail: tshamim@masdar.ac.ae

Received 25 September 2011; Revised 28 February 2012; Accepted 2 March 2012

1. INTRODUCTION

The performance of a fuel cell, which is a promising energy-efficient and environment-friendly technology, is significantly influenced by humidification level of reactants (mainly of air). The effect of humidification is particularly stronger in hot regions and at high operating temperatures. The effect is caused by changes in cell reaction thermodynamics and kinetics, mass transfer, membrane conductivity, and reactant partial pressures. An optimum level of humidification is required for the high performance of fuel cell. The fuel cell performance is deteriorated if the humidification level is below or above its optimum level because a higher level may cause electrode flooding, and a lower level may result in the reduction of the membrane's proton conductivity [1]. Because the humidification requirement varies with the fuel cell operating conditions, maintaining a proper humidification level is more challenging under transient conditions.

Because of its importance, many researchers have investigated the effect of humidity level on the fuel cell performance and have generated some good understanding under steady state conditions. However, the effect of humidity on the fuel cell operation under transient operating conditions is not well understood.

Jang *et al.* [2] investigated the influence of inlet relative humidity of reactant gases on both anode and cathode on the cell performance and transport phenomenon with baffle-blocked flow field designs and showed that the cell performance declines with a decrease in relative humidity. Xu *et al.* [3] showed that the reduced relative humidity increases the polarization losses, membrane and electrode resistance, cathode activation loss and oxygen transport loss, by affecting the membrane and electrode ionic resistance, catalytic activity and oxygen transport. They reaffirmed that the control of the relative humidity is crucial to improve the performance of fuel cell and to avoid permanent damage to the membranes. The ideal operational condition is relative humidity in saturated conditions [4]. Ahn *et al.* [5] studied the effect of humidity on the performance of a polymer electrolyte membrane (PEM) fuel cell.

Guvelioglu and Stenger [6] showed that the humidification affects the current and power densities, membrane dry-out, and electrode flooding. In another study, Jeong *et al.* [7] found that the cell performance was improved with increasing relative humidity of atmosphere in the

low current region and lowered in high current region. Saleh *et al*. [8] studied the interlinked effects of symmetric relative humidity and asymmetric relative humidity on the performance of H_2/air PEM fuel cell at different temperatures. The effect of relative humidity on PEM fuel cell performance was studied at elevated temperatures under ambient backpressure by Zhang *et al*. [9], and their results showed that fuel cell performance could be depressed significantly by decreasing relative humidity from 100% to 25%. Reducing relative humidity can result in slower electrode kinetics, including electrode reaction and mass diffusion rates, and higher membrane resistance. Zhang *et al*. [10] investigated the effects of cathode inlet humidification on PEM fuel cell load change operations and the fuel cell performance during a simulated start-up process. The results showed that an increase in the cathode inlet humidification significantly influences the start-up performance of a PEM fuel cell. The cathode inlet relative humidity under 30% significantly dropped the cell dynamic performance.

Using a three-dimensional model, Wang and Wang [11,12] studied the effect of step increase in current density, cell voltage and humidity on the PEM fuel cell dynamic performance. They estimated time constant for membrane hydration. Guilin *et al*. [13] investigated the effect of time-varying relative humidity (through step and sinusoidal changes with relative humidity varying between 80% and 100%) on the performance of PEM fuel cell. They found that decreasing (increasing) the humidity value results in the increase (decrease) of the average current density. However, there was no significant effect on the temperature, which changed by only 0.1 K. The cell response was symmetrical around the initial steady-state value.

A critical review of the past studies indicates that there are few investigations on the effect of variable humidity conditions. Variable humidification levels may be required for a fuel cell if it is operating under transient conditions or if the ambient air humidity is changed. Furthermore, if the fuel cell humidifier malfunctions, the humidification levels of the reactants may vary. The present study was motivated by realizing the gap in literature and the need for better understanding of the effect of variable humidity on the fuel cell performance. It investigates the effect of time-varying relative humidity on the PEM fuel cell's current and power densities and water distribution in electrodes by employing a mathematical model. The novelty of the model, presented in Vorobev *et al*. [14], is that it does not rely on the non-physical assumption of the uptake curve equilibrium between the pore vapor and ionomer water in the catalyst layers. Instead, the transition between the two phases is modeled as a finite-rate equilibration process.

2. MATHEMATICAL FORMULATION

A PEM fuel cell consists of porous anode and cathode diffusive layers, membrane, anode catalyst layer (ACL) and cathode catalyst layer (CCL). The current study is not focused on the channel flow, and accordingly, the mathematical model does not include the anode and cathode gas channels. However, the channel effects are captured by the boundary conditions, which are specified at the borders of the anode and cathode. Considering the focus of the present work, a one-dimensional, transient approach is taken, with all fields being functions of the coordinate x across the cell and time t. Using the assumptions and notations listed elsewhere[14], the governing equations for the five components of fuel cell may be written as shown in Table I.

In contrast to other existing models, the present model does not rely on the non-physical assumption of the uptake curve equilibrium between the pore vapor and ionomer water in the catalyst layers. Instead, the transition between the two phases is modeled as a finite-rate equilibration process by employing a phenomenological parameter γ, which has the physical meaning of the non-dimensional reciprocal equilibration time. The parameter γ is varied between 100 (almost immediate equilibration) and 0.1 (very slow equilibration).

The water content in the membrane was assumed to be initially in equilibrium with the vapor concentration. All the boundary and initial conditions, and physical quantities used in simulations are similar to those listed in reference [14]. The system of governing equations is solved by the finite-difference method. The second-order central discretization formulas were used for spatial discretization, and the Runge–Kutta method of second order is used for the temporal integration. The spatial node size varied in each sub-domain ranging from 1.5×10^{-5} m for the anode/cathode, 2.55×10^{-6} m for the membrane, and 5×10^{-7} m for the catalyst layers. The time step was constant and equal to 4×10^{-7}. The grid insensitivity of results was ensured by performing a sensitivity study. Details of the solution procedure are described elsewhere [14].

The modulating relative humidity conditions were simulated by using the following sinusoidal input:

$$RH(t) = RH_{mean} \times (1 + A \times \sin(2\pi f t))$$

where A is amplitude and f is frequency of the modulations. The mathematically smooth sinusoidal function was selected to represent the transients because this function allows better understanding of the fuel cell response to the imposed modulation in terms of its amplitude and frequency, and ease in comparison with experimental and analytical results. For these reasons, many past studies used sinusoidal changes to simulate transient conditions [15,16].

3. RESULTS AND DISCUSSION

The numerical model was validated by comparing the polarization curve of the present model with the experimental results of Liu *et al*. [17], as shown in Figure 1. The figure shows a good agreement between the simulation and experimental results, particularly at low current density values. The numerical model was also validated by comparing with

Int. J. Energy Res. 2013; **37**:1223–1231 © 2012 John Wiley & Sons, Ltd.
DOI: 10.1002/er

Table I. Governing equations for the fuel cell.

Anode and cathode gas diffusion layers	
Conservation of mass	$\varepsilon\frac{\partial\rho}{\partial t}+\frac{\partial}{\partial x}(\rho u)=0$
Conservation of momentum	$\frac{\partial p}{\partial x}=-\frac{\mu}{K}u$
Species conservation equation (for H_2 and O_2)	$\varepsilon\frac{\partial}{\partial t}C^{X}+\frac{\partial}{\partial x}(uC^{X})=\frac{\partial}{\partial x}\left(D_{eff}^{X}\frac{\partial}{\partial x}C^{X}\right)$
Species conservation equation for H_2O	$\varepsilon\frac{\partial}{\partial t}C^{H_2O}+\frac{\partial}{\partial x}(uC^{H_2O})=\frac{\partial}{\partial x}\left(D_{eff}^{H_2O}\frac{\partial}{\partial x}C^{H_2O}\right)$
Equation of state	$p=RT\left(C^{X}+C^{H_2O}+C^{N_2}\right)$
Mixture density	$\rho=M^{X}C^{X}+M^{H_2O}C^{H_2O}+M^{N_2}C^{N_2}$
Anode catalyst layer (ACL) and cathode catalyst layer (CCL)	
Conservation of mass	$\varepsilon\frac{\partial\rho}{\partial t}+\frac{\partial}{\partial x}(\rho u)=-M^{X}\frac{1}{2F}j-M^{H_2O}\gamma^{*}\left(p_m\lambda_e-C_\lambda^{H_2O}\right)$
Conservation of momentum	$\frac{\partial p}{\partial x}=-\frac{\mu}{K}u$
Species conservation equation (for H_2 and O_2)	$\varepsilon\frac{\partial}{\partial t}C^{X}+\frac{\partial}{\partial x}(uC^{X})=\frac{\partial}{\partial x}\left(D_{eff}^{X}\frac{\partial}{\partial x}C^{X}\right)-\frac{1}{ZF}j$ ($Z=2$ for ACL and 4 for CCL)
Species conservation equation for H_2O	$\varepsilon\frac{\partial}{\partial t}C^{H_2O}+\frac{\partial}{\partial x}(uC^{H_2O})=\frac{\partial}{\partial x}\left(D_{eff}^{H_2O}\frac{\partial}{\partial x}C^{H_2O}\right)-\gamma^{*}\left(p_m\lambda_e-C_\lambda^{H_2O}\right)$
Equation of state	$p=RT\left(C^{X}+C^{H_2O}+C^{N_2}\right)$
Mixture density	$\rho=M^{X}C^{X}+M^{H_2O}C^{H_2O}+M^{N_2}C^{N_2}$
Charge conservation equation	$\frac{\partial}{\partial x}\left(\kappa_{eff}\frac{\partial\Phi}{\partial x}\right)+j=0$
Liquid water transport equation for **ACL**	$m\frac{\partial}{\partial t}C_\lambda^{H_2O}=\frac{\partial}{\partial x}\left(D_{m,eff}^{H_2O}\frac{\partial}{\partial x}C_\lambda^{H_2O}\right)-\frac{n_d}{F}j+\gamma^{*}\left(p_m\lambda_e-C_\lambda^{H_2O}\right)$
Liquid water transport equation for **CCL**	$\frac{\partial}{\partial t}C_\lambda^{H_2O}=\frac{\partial}{\partial x}\left(D_{m,eff}^{H_2O}\frac{\partial}{\partial x}C_\lambda^{H_2O}\right)-\frac{1}{F}\left(\frac{1}{2}+n_d\right)j+\gamma^{*}\left(p_m\lambda_e-C_\lambda^{H_2O}\right)$
Transfer current equation for **ACL**	$j=j_a(C^{H_2})^{1/2}\Phi;\ j_a\equiv j_{ref}^{a}\left(C_{ref}^{H_2}\right)^{-1/2}\frac{\alpha_a+\alpha_c}{RT}F$
Transfer current equation for **CCL**	$j=j_cC^{O_2}\exp(\alpha\Phi);\ j_c=j_{ref}^{c}\left(C_{ref}^{O_2}\right)^{-1}\exp\left(\frac{\alpha_cF}{RT}(V_{cell}-V_0)\right);\ \alpha=\frac{\alpha_cF}{RT}$
Membrane	
Equation for diffusion of liquid water	$\frac{\partial}{\partial t}C_\lambda^{H_2O}=\frac{\partial}{\partial x}\left(D_m\frac{\partial}{\partial x}C_\lambda^{H_2O}\right)$
Charge conservation equation	$\frac{\partial}{\partial x}\left(\kappa\frac{\partial\Phi}{\partial x}\right)=0$

$X = H_2$ for anode and ACL; $X = O_2$ for cathode and CCL

the results of a three-dimensional model of Wang and Wang [18] as reported in our previous paper [14]. The validation results showed the suitability of the present model in simulating the performance of fuel cell. The fuel cell geometry and operating conditions are similar to that reported in our previous paper [14].

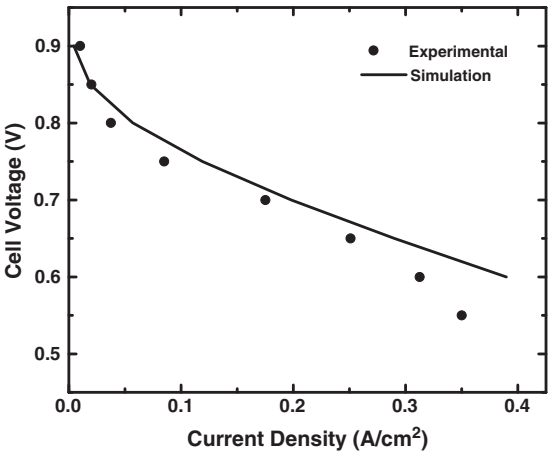

Figure 1. Experimental validation of the model: comparison of polarization curve with the experimental results of Liu *et al.* [17].

The positive effect of relative humidity on the water distribution, current and power densities during steady state conditions is well understood. In the present study, we investigated the effect of time-varying modulating values of relative humidity on the fuel cell's performance. This was performed by considering a steady operating fuel cell at 0.7 V, which was suddenly subjected to sinusoidal variations of relative humidity. During these oscillations, other inlet operating conditions remained unchanged. Figure 2 shows the results of the imposed sinusoidal modulation in relative humidity, initially set at 50% relative humidity, with a frequency of 1 Hz and amplitude of 10%, and $\gamma = 100$. The modulation causes the relative humidity to vary between 25% and 75% during each modulation period.

Figure 2 shows that the current and power densities respond sinusoidally to the imposed sinusoidal relative humidity modulation. Similar to the steady state behavior, the current and power densities increase with an increase in relative humidity. The values follow the sinusoidal pattern of the modulating relative humidity and attain the maximum and minimum, corresponding to the peak and trough values of the relative humidity. The response amplitude (defined as the difference of peak and trough values divided by the steady-state value corresponding to the mean relative humidity) is small and is equal to 4.3%.

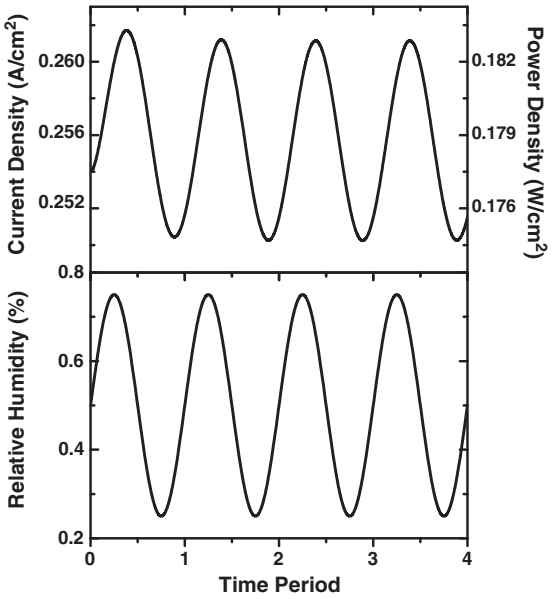

Figure 2. Effect of relative humidity modulations on the fuel cell current and power densities (modulation frequency = 0.1 Hz, modulation amplitude = 50%, relaxation parameter (γ) = 100): (a) current and power densities; (b) imposed relative humidity modulation.

The maximum and minimum values of current and power densities for modulating conditions are different from their steady-state values corresponding to the peak and trough values of the relative humidity. The difference of the maximum and minimum values of current (and power) density for the modulating condition is 6.16% of the corresponding difference for the steady state case.

Figure 3 shows the average liquid water content (λ) (which is defined as the number of water molecules per sulfonic-acid group) in the membrane and the anodic and cathodic catalyst layers, which also responds sinusoidally to the imposed modulation. Similar to the steady state behavior, (λ) in the membrane and catalyst layers increases with an increase of relative humidity. Its values follow the sinusoidal pattern of the modulating relative humidity and attain the maximum and minimum values corresponding to the peak and trough values of the relative humidity. However, there is phase lag in (λ)'s response to the imposed modulation. The phase lag is relatively greater for (λ) in the membrane. The response amplitude is 16.2% and 15.2% for anodic and cathodic catalyst layers, respectively, whereas the response amplitude for membrane is very small (1.3%). The difference of the maximum and minimum values of (λ) for the modulating condition is 17.4%, 12.84% and 1.34% of the corresponding difference for the steady state case for anodic and cathodic catalyst layers, and membrane, respectively.

Figure 4 shows the effect of modulating relative humidity on the average vapor concentrations (expressed in non-dimensional form as RTC^{H2O}/p_{sat}) in anode and cathode, which also respond sinusoidally. As expected, the

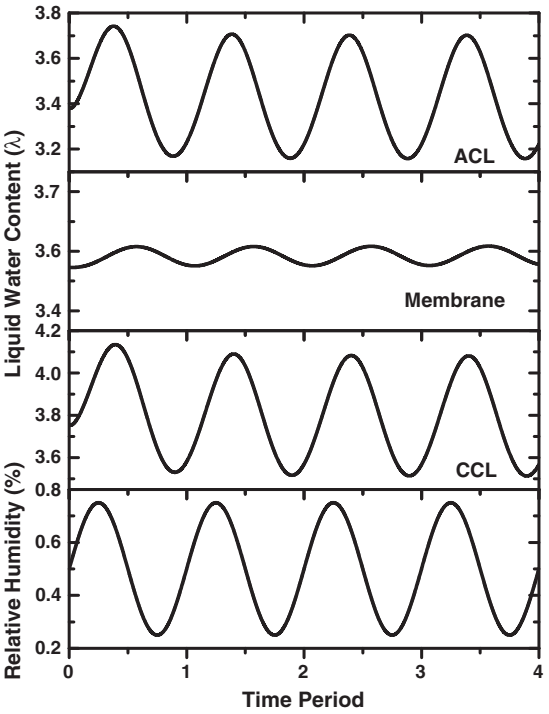

Figure 3. Effect of relative humidity modulations on the average liquid water content (modulation frequency = 0.1 Hz, modulation amplitude = 50%; relaxation parameter (γ) = 100): (a) anodic catalyst layer; (b) cell membrane; (c) cathodic catalyst layer; (d) imposed relative humidity modulation.

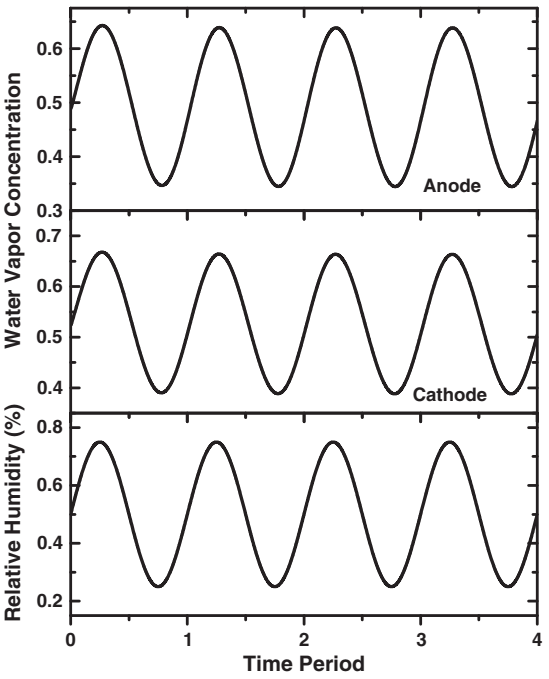

Figure 4. Effect of relative humidity modulations on the water vapor content (modulation frequency = 0.1 Hz, modulation amplitude = 50%; relaxation parameter (γ) = 100): (a) anode; (b) cathode; (c) imposed relative humidity modulation.

Int. J. Energy Res. 2013; **37**:1223–1231 © 2012 John Wiley & Sons, Ltd.
DOI: 10.1002/er

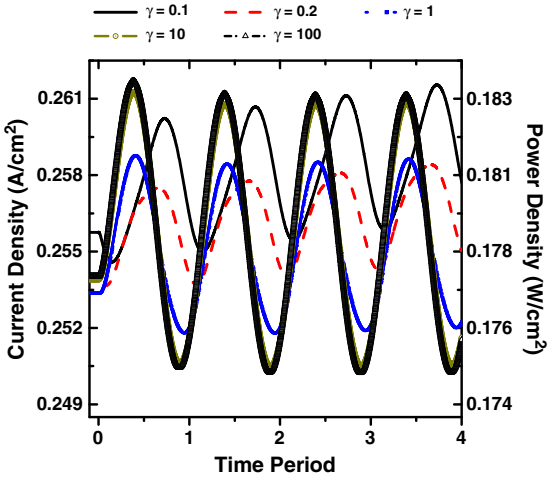

Figure 5. Effect of relaxation parameter (γ) on the on the fuel cell current and power density response to modulations in relative humidity (modulation frequency = 0.1 Hz; modulation amplitude = 50%).

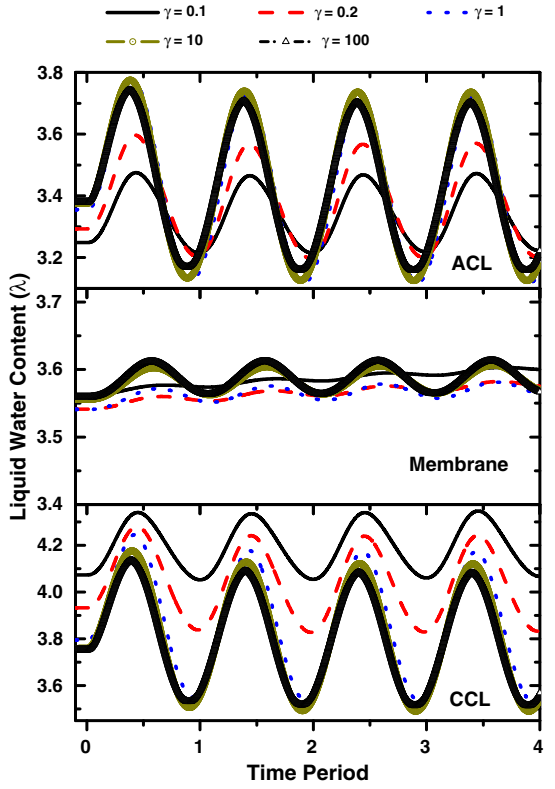

Figure 6. Effect of relaxation parameter (γ) on the cell average liquid water content response to modulations in relative humidity (modulation frequency = 0.1 Hz; modulation amplitude = 50%): (a) anodic catalyst layer; (b) cell membrane; (c) cathodic catalyst layer.

response amplitude is high and is 60% and 52.7% for anode and cathode, respectively. The difference of maximum and minimum values of vapor concentration in anode and cathode for the modulating condition are 59.47% and 54.61%, respectively, of the corresponding differences for the steady state case.

3.1. Effect of relaxation parameter γ

Figures 5–7 show the effect of relaxation parameter (γ) on the fuel cell current and power densities and water distribution during transient conditions. These results were obtained by considering sinusoidal modulation in relative humidity with a frequency of 0.1 Hz and amplitude of 50% and various values of γ (0.1, 0.2, 1, 10 and 100). The results show that the cell response remains sinusoidal, and the value of γ mainly affects the mean value and the cell response amplitude.

Figure 5 shows that the mean values about which the current and power densities oscillate increase with increasing values of γ. An increase of γ also increases the mean value of (λ) in anodic catalyst layer; however, it has opposing effect on (λ) in cathodic catalyst layer (Figure 6). The increase of γ increases the response amplitude for current and power densities and (λ) in catalyst layers, but it decreases the response amplitude of water vapor concentrations in anode and cathode (Figure 7). However, the

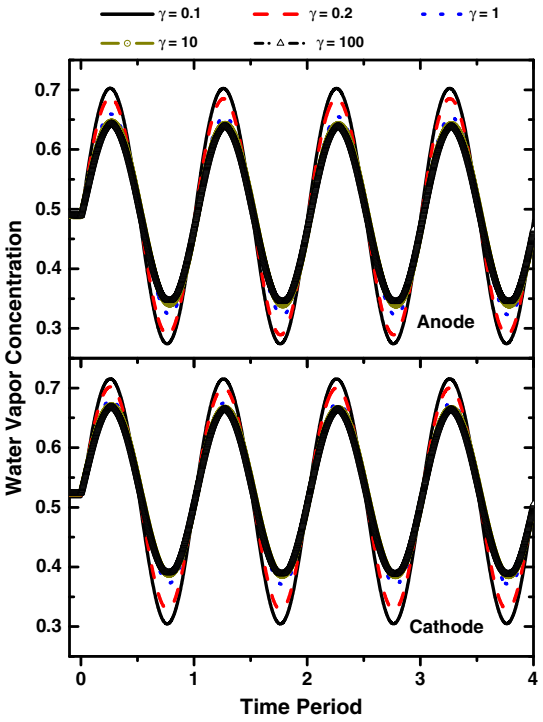

Figure 7. Effect of relaxation parameter (γ) on the cell water vapor content response to modulations in relative humidity (modulation frequency = 0.1 Hz, modulation amplitude = 50%): (a) anode; (b) cathode.

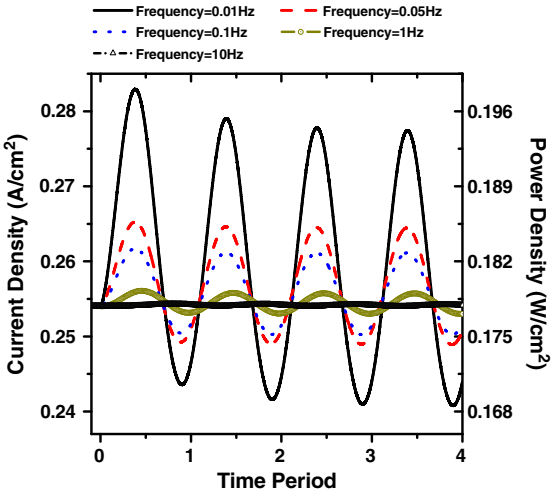

Figure 8. Effect of modulation frequency on the fuel cell current and power density response to modulations in relative humidity (modulation amplitude = 50%; relaxation parameter (γ) = 100).

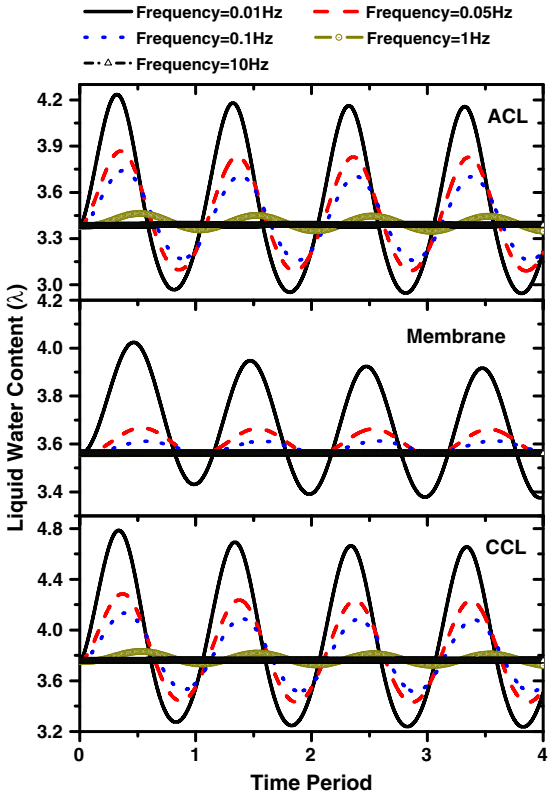

Figure 9. Effect of modulation frequency on the cell average liquid water content response to modulations in relative humidity (modulation amplitude = 50%; relaxation parameter (γ) = 100): (a) anodic catalyst layer; (b) cell membrane; (c) cathodic catalyst layer.

effect of γ disappears at higher values. For example, there is no significant difference between the responses for $\gamma = 10$ and $\gamma = 100$.

3.2. Effect of modulation frequency

The effect of modulation frequency was investigated by considering relative humidity modulations with different frequencies. The results presented (Figures 8–10) are for fuel cell, initially operating at a cell voltage of 0.7 V with $\gamma = 100$, and subjected to sinusoidal oscillation in relative humidity of 50% amplitude. It should be noted that realistic changes in humidification levels may not involve frequencies higher than 1 Hz. However, the higher frequency cases were included in this study to verify the response trends. The results depict, as expected, that the cell response to imposed oscillation is maximum at low frequencies, and the response amplitude decreases and deviates from the corresponding steady-state values as the modulating frequency increases. At higher frequencies, the cell's current and power densities, liquid and vapor contents become insensitive to imposed relative humidity modulations. The cut-off frequency corresponding to the current and power densities and (λ)'s insensitivity to the imposed modulations is approximately 10 Hz. The vapor content response remains sensitive to the imposed modulation up to 100 Hz (owing to computational limitations, frequencies above 100 Hz were not investigated). Higher frequencies also increase the initial phase lag in the cell response to imposed modulations. Similar results are obtained for other values of γ.

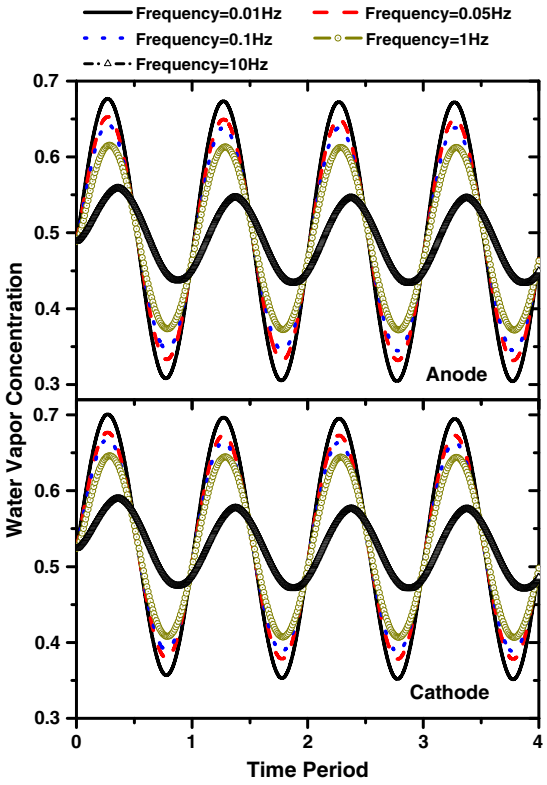

Figure 10. Effect of modulation frequency on the cell water vapor content response to modulations in relative humidity (modulation amplitude = 50%, relaxation parameter (γ) = 100): (a) anode; (b) cathode.

Int. J. Energy Res. 2013; **37**:1223–1231 © 2012 John Wiley & Sons, Ltd.
DOI: 10.1002/er

3.3. Effect of modulation amplitudes

Figures 11–13 show the cell's current and power densities, liquid water content (λ) and water vapor concentration

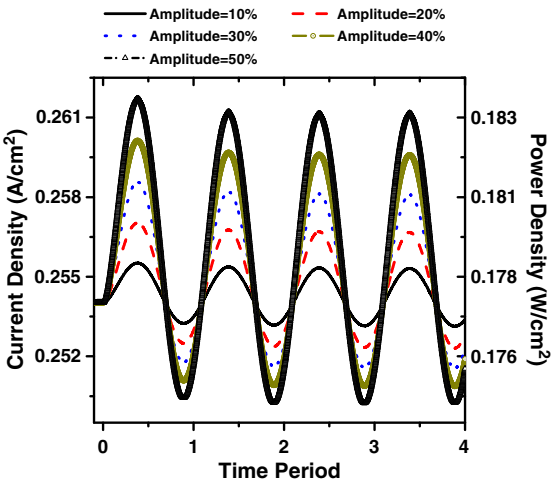

Figure 11. Effect of modulation amplitude on the fuel cell current and power density response to modulations in relative humidity (modulation frequency = 0.1 Hz; relaxation parameter (γ) = 100).

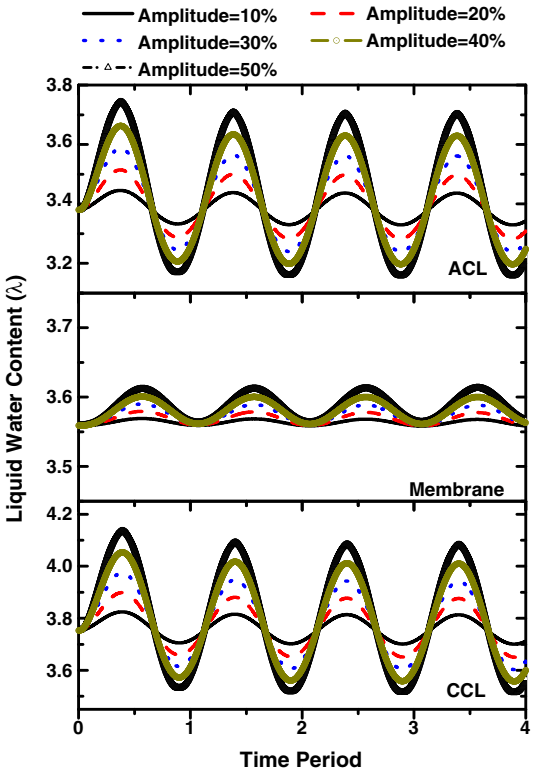

Figure 12. Effect of modulation amplitude on the cell average liquid water content response to modulations in relative humidity (modulation frequency = 0.1 Hz; relaxation parameter (γ) = 100): (a) anodic catalyst layer; (b) cell membrane; (c) cathodic catalyst layer.

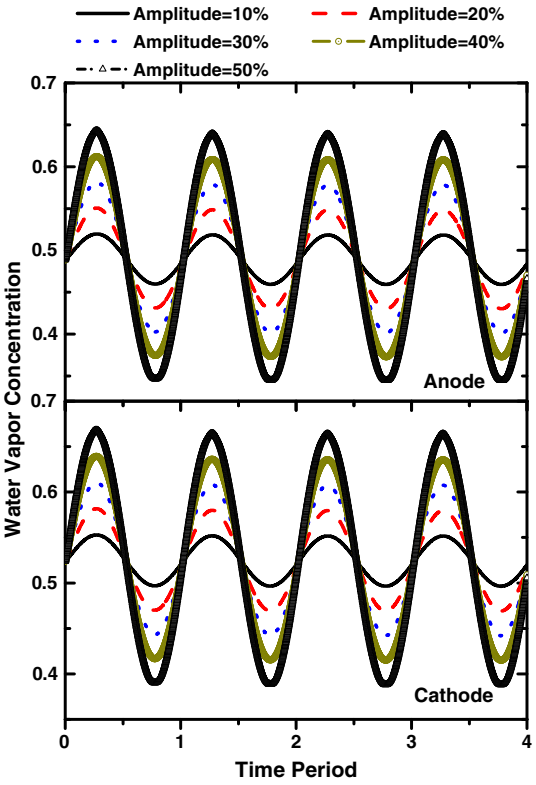

Figure 13. Effect of modulation amplitude on the cell water vapor content response to modulations in relative humidity (modulation frequency = 0.1 Hz; relaxation parameter (γ) = 100): (a) anode; (b) cathode.

responses for different amplitudes of relative humidity modulations. These results are for fuel cell, initially operating at a cell voltage of 0.7 V and $\gamma = 100$, which is subjected to sinusoidal oscillation in relative humidity of 0.1 Hz frequency for various amplitudes (10%, 20%, 30%, 40% and 50%). The results depict that the increase in oscillation amplitude increases the cell response. For all modulation amplitudes, the cell response remains sinusoidal. The increase of modulation amplitude increases the mean value around, which the current (and power) density responds. For the conditions studied, other than the response amplitude, the modulation amplitude has insignificant influence on any other aspect of the cell water response. Similar results are obtained for other values of γ, except that the effect of modulation amplitude is relatively less for lower γ.

4. CONCLUSIONS

By employing a numerical model, this study investigated the effect of modulating relative humidity on the fuel cell's current and power densities and water distribution in electrodes and membrane. The model considers a finite-rate equilibration process between the pore vapor and

ionomer water in the catalyst layers by employing a phenomenological parameter γ, which has the physical meaning of the non-dimensional reciprocal equilibration time. The study was conducted with a range of γ values from 0.1 to 100, with the higher value of γ representing the fast equilibration. The results led to the following conclusions:

- The fuel cell's current and power densities and water distribution respond to variation in relative humidity. The response is sinusoidal to the sinusoidal imposed modulation. As expected, the modulation of relative humidity has greater effect on water distribution than that on the power and current densities. The response values for the modulating conditions are different from the corresponding steady-state values. In general, γ mainly affects the mean value and the cell response amplitude. An increase of γ increases the response amplitude (and sensitivity) of current and power densities and liquid content, but it decreases the response amplitude of vapor concentrations.
- The modulating frequency affects the cell response to the imposed changes. The cell response is maximum at low frequencies, and it decreases with an increase of modulation frequencies. At high frequencies, the cell becomes insensitive to the imposed relative humidity modulations. The current and power densities and liquid water content become insensitive to the imposed modulations occurs at approximately 10 Hz. However, the vapor content remains sensitive to the imposed modulation up to 100 Hz.
- The response amplitude increases with an increase of modulation amplitude for all values of γ. The increase of modulation amplitude increases the mean value around which the current and power densities respond. The effect of modulation amplitude is relatively less for lower values γ.

NOMENCLATURE

a	= vapor activity
A	= modulation amplitude
C^k	= molar concentration of species k (mol/m^3)
D^k	= diffusivity of species k in gas mixture (m^2/s)
EW	= equivalent weight of ionomer (kg/mol)
f	= modulation frequency (Hz)
F	= Faraday's constant (96 487 Col)
i	= current density (A/cm^2)
j	= transfer current (A/m^2)
K	= permeability (m^2)
L	= thickness of cell (m)
L_c	= thickness of catalyst layer (m)
m	= volume fraction of ionomer in catalyst layer
M^k	= molar weights of species k (kg/mol)
n_d	= electro osmotic drag coefficient (H_2O/H^+)
p	= pressure (Pa)
R	= gas constant (8.314 J/mol K)
RH	= relative humidity
t	= time (s)
T	= temperature (K)
u	= filtration velocity (m/s)
V	= voltage (V)

Greek symbols

α	= transfer coefficient
ε	= porosity
Φ	= phase potential (V)
γ	= relaxation parameter
κ	= ionic conductivity (A/Vm)
λ	= membrane water content
ρ	= density (kg/m^3)
τ_g	= gas diffusion time of the reactant gases (s)
τ_γ	= relaxation (equilibration) time (s)
ξ	= stoichiometric flow rate

Subscripts and superscripts

a	= anode
c	= cathode
cell	= cell
e	= equilibrium
eff	= effective value
k	= species
m	= membrane phase
max	= maximum
ref	= reference
sat	= saturated value

ACKNOWLEDGEMENT

The financial supports from the HP-Center for Engineering Education and Practice (HP-CEEP) of the University of Michigan-Dearborn and the Government of Abu Dhabi are greatly appreciated.

REFERENCES

1. Larminie J, Dicks A. *Fuel Cell Systems Explained*, 2nd ed., John Wiley & Sons: Chichester, England, 2003.
2. Jang J-H, Yan W-M, Li H-Y, Chou Y-C. Humidity of reactant fuel on the cell performance of PEM fuel cell with baffle-blocked flow field designs. *Journal of Power Sources* 2006; **159**:468–477.
3. Xu H, Kunz HR, Fenton JM. Analysis of proton exchange membrane fuel cell polarization losses at elevated temperature 120 °C and reduced relative humidity. *Electrochimica Acta* 2007; **52**:3525–3533.
4. Riascos LAM, Simoes MG, Miyagi PE. Controlling PEM fuel cells applying a constant humidity technique. *ABCM Symposium Series in Mechatronics* 2008; **3**:774–783.

Int. J. Energy Res. 2013; **37**:1223–1231 © 2012 John Wiley & Sons, Ltd.
DOI: 10.1002/er

5. Ahn S-Y, Lee Y-C, Ha HY, Hong S-A, Oh I-H. Effect of the ionomers in the electrode on the performance of PEMFC under non-humidifying conditions. *Electrochimica Acta* 2004; **50**:673–676.
6. Guvelioglu GH, Stenger HG. Flow rate and humidification effects on a PEM fuel cell performance and operation. *Journal of Power Sources* 2007; **163**: 882–891.
7. Jeong SU, Chob EA, Kim H-J, Lim T-H, Oh I-H, Kima SH. Effects of cathode open area and relative humidity on the performance of air-breathing polymer electrolyte membrane fuel cells. *Journal of Power Sources* 2006; **158**:348–353.
8. Saleh MM, Okajima T, Hayase M, Kitamura F, Ohsaka T. Exploring of effects of symmetrical and asymmetrical relative humidity on the performance of H2/air PEM fuel cell at different temperatures. *Journal of Power Sources* 2007; **164**: 503–509.
9. Zhang J, Tang Y, Song C, Xia Z, Li H, Wang H, Zhang J. PEM fuel cell relative humidity (RH) and its effect on performance at high temperatures. *Electrochimica Acta* 2008; **53**:5315–5321.
10. Zhang Z, Jia L, Wang X, Ba L. Effects of inlet humidification on PEM fuel cell dynamic behaviours. *International Journal of Energy Research* 2011; **35**:376–388.
11. Wang Y, Wang C-Y. Transient analysis of polymer electrolyte fuel cells. *Electrochemica Acta* 2005; **50**:1307–1315.
12. Wang Y, Wang C-Y. Dynamics of polymer electrolyte fuel cells undergoing load changes. *Electrochemica Acta* 2006; **51**:3924–3933.
13. Guilin H, Jianren T. Transient computation fluid dynamics modeling of a single proton exchange membrane fuel cell with serpentine channel. *Journal of Power Sources* 2007; **165**:171–184.
14. Vorobev A, Zikanov O, Shamim T. A computational model of a PEM fuel cell with finite vapor absorption rate. *Journal of Power Sources* 2007; **166**:92–103.
15. Hu G, Fan JR. Transient computation fluid dynamics modeling of a single proton exchange membrane fuel cell with serpentine channel. *Journal of Power Sources* 2007; **165**:171–184.
16. Haddad A, Bouyekhf R, El Moudni A. Dynamic modeling and water management in proton exchange membrane fuel cell. *International Journal of Hydrogen Energy* 2008; **33**:6239–6252.
17. Liu Z, Mao Z, Wang C, Zhuge W, Zhang Y. Numerical simulation of a mini PEMFC stack. *Journal of Power Sources* 2006; **160**:1111–1121.
18. Wang Y, Wang C-Y. Modeling polymer electrolyte fuel cells with large density and velocity changes. *Journal of the Electrochemical Society* 2005; **152**:A445–A453.